The Techno-Economic Viability of Actively Supported Structures for Terrestrial Transit and Space Launch

Philip Swan
The Atlantis Project
philswan@project-atlantis.com

Abstract— **A Tethered Ring is a dynamic structure that can cost-effectively support carbon-neutral transportation and space launch infrastructure at high altitudes. The capital cost per available seat kilometer, amortized over 20 years, is estimated to be 0.00121 USD/km. The levelized cost-per-kg launched to nearby planets, moons, and asteroids is estimated at 12.45 USD/kg when amortized over 1.5 million metric tons of payload launched on interplanetary trajectories.**

A Tethered Ring is constructed exclusively with materials that are mass-produced today and it makes use of technologies and physics that are widely used in other industries and well understood from an engineering standpoint. It generates one component of its lifting force using cables called "tethers" and another component by using a fast-moving magnetically confined mass stream within an evacuated tube. The architecture enables the mass-stream to be confined with minimal magnetic friction, giving it a significant operating cost advantage over earlier concepts such as orbital rings, space cables, and launch loops.

TABLE OF CONTENTS

1. INTRODUCTION

High-altitude transit and electromagnetic launch systems, held aloft by a Tethered Ring, provide a low-cost, carbon-neutral alternative to commercial aviation and chemical rockets.

This paper assesses these systems' technical, economic, environmental, and geopolitical viability by using a multi-faceted approach. Technical viability is assessed by comparing each component and sub-system of the architecture to a similar technology called a "heritage technology" that already exists and is in use. Economic viability is established by estimating key systems performance metrics such as the capital cost per available seat kilometer for transportation services, and the launch cost-per-kilogram to destinations such as the Moon, Mars, Venus, and the asteroids. Environmental viability is addressed by, for example, explaining how systems are powered by renewable energy sources. The geopolitical viability is assessed by discussing options that require various levels of international collaboration and that come with different amounts of geopolitical risk. The geopolitics section also explores the architecture's resilience to terrorism and the failure scenario.

2. BACKGROUND

A Tethered Ring[1], [2] is an Inertially Supported Active Structure. It is energy efficient and easier to build with contemporary materials and technologies. The quintessential tethered ring employs a constant length, constant gravitational potential, and constant lateral acceleration mass stream; therefore, the mass stream does not need discrete units of mass, expansion joints, or a similar feature that would cause it to be less than perfectly homogeneous in its direction of travel. Imperfections in "axial homogeneity" disturb the magnetic fields that confine the mass stream and induce eddy currents, a primary source of magnetic friction. The architecture also minimizes changes in the lateral acceleration applied to the mass stream which is another source of changing magnetic fields that can result in both eddy current losses and magnetic hysteresis losses[3].

In normal operation, the kinetic energy of the Tethered Ring's mass streams is kept constant; therefore, operating the device does not involve cycling the mass streams' energy through linear motors and linear generators, which would convert some of the energy to heat.

Earlier concepts that have been proposed in the literature for implementing an Inertially Supported Active Structure include the General Planetary Vehicle (GPV)[4], the Full Standard Orbital Ring System (FSORS)[5], the Partial Orbital Ring System (PORS)[5], the Lofstrom Loop (LL)[6], the Space Cable (SC)[7][8], and the Hyde design for a Space Fountain (HSF)[9]. Table 1 compares the energy efficiency attributes of the Tethered Ring (TR) to these other proposed concepts.

Table 1: Comparison of the attributes of inertially supported active structures that affect mass-stream energy consumption

	Axially Homogeneous Mass Stream	Constant Lateral Acceleration	Constant Energy Mass Stream
GPV	No	**Yes**	No
FSORS	No	No	**Yes**
PORS	No	No	**Yes**
LL	No	No	**Yes**
SC	No	No	**Yes**
HSF	No	No	No
TR	**Yes**	**Yes**	**Yes**

978-1-6654-9032-0/23/$31.00 ©2023 IEEE

Notes: 1) If the proposal, as described in the referenced literature, employs a mass stream that locally changes in length, and if either discrete mass elements or some form of mass stream expansion joint technology is described, then the technology is deemed to not to have an "axially homopolar mass stream". 2) If the mass stream is diverted significantly more in some places than in others, then it does not have "constant lateral acceleration". 3) If the system uses linear motors and generators to actively accelerate and decelerate any portion or portions of the mass stream when it is in operation, as opposed to just maintaining its speed by countering energy losses due to friction, then the energy of the mass stream is not constant.

Variants of the Tethered Ring are possible, so long as the variations are not so great that they wholly negate the fundamental advantages of the architecture. For example, a variant may be less than perfectly circular to increase the number of people that it can serve (aka, its catchment zone) with its transit system. A variant may climb and descend to different altitudes around its circumference so that it can support different systems at different altitudes. For example, a launcher may benefit from a higher altitude and may be able to justify a higher cost per kg supported, while a lower altitude may be more optimal for a terrestrial transit system. A variant may accelerate and decelerate its mass streams during operation by small amounts for grid-scale energy storage and energy transmission purposes. The moving rings of a tethered ring variant may be designed to support small amounts of axial deformation within the strain limits of their material without compromising their axial homogeneity from a magnetic field perspective.

3. TECHNICAL FEASIBILITY

There are many components of the system for which technical feasibility needs to be assessed. To provide a mathematical basis for subsequent discussions, our analysis starts by focusing on a reference design that masses 100kg per meter, has a radius of 5220km, and operates on Earth at an altitude of 32km. These are not necessarily the most optimal design choices - they simply represent a useful starting point for analysis.

To begin, let us consider the "distilled" problem of a tethered ring that is not supporting any facilities with dynamic loads (such as a transit system) and where the environmental and societal circumstances are ideal. Discussions about construction, routine maintenance, defense, etc. will be covered in later sections of this paper or have already been covered in earlier referenced work. Our first goal will be to mathematically derive useful baseline metrics, such as materials cost and operating costs per kg of facilities supported at the operational altitude.

The force of gravity acting on a 1m long portion of the ring is...

$$|\boldsymbol{F}_G| = \frac{GM_P m_r}{(r_P + h_r)^2} \quad (1)$$

Where:
'$\boldsymbol{F}_G$' is a vector representing the force of gravity
'G' is the gravitational constant
'M_P' is the mass of the planetary body
'm_r' is the mass per meter of ring
'r_P' is the radius of the planetary body
'h_r' is the operational altitude of the ring

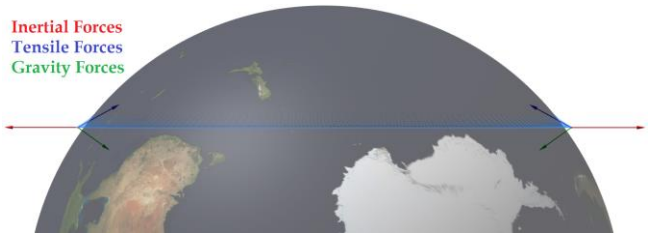

Figure 1: Outwards inertial forces (red), tensile forces (blue), and downward gravity forces (green)

Let us center the ring on the origin of a cylindrical coordinate system {ρ, ϕ, z} such that the direction of the positive z-axis is away from the center of the planetary body. In this coordinate system, we can see that none of the forces have a ϕ-component. The gravity forces have a negative ρ-component and a negative z-component. The inertial forces have a positive ρ-component, but no z-component. The tensile forces have a negative ρ-component and a positive z-component.

Since we know 'r_P', 'h_r', and 'r_r' (the radius of the ring) we can use trigonometry to determine $F_{\rho,G}$ and $F_{z,G}$.

$$F_{\rho,G} = -|\boldsymbol{F}_G|\frac{r_r}{r_P + h_r} \quad (2)$$

$$F_{z,G} = -|\boldsymbol{F}_G|\frac{\sqrt{(r_P + h_r)^2 - r_r^2}}{r_P + h_r} \quad (3)$$

To support the ring against the pull of gravity, each inertial force vector and tensile force vector must combine to cancel out each gravity force vector.

$$\boldsymbol{F}_I + \boldsymbol{F}_T = -\boldsymbol{F}_G \quad (4)$$

Rearranging...

$$\boldsymbol{F}_I + \boldsymbol{F}_T + \boldsymbol{F}_G = 0 \quad (5)$$

Component versions of these equations are...

$$F_{\rho,I} + F_{\rho,T} + F_{\rho,G} = 0 \quad (6)$$

$$F_{\phi,I} + F_{\phi,T} + F_{\phi,G} = 0 \quad (7)$$

$$F_{z,I} + F_{z,T} + F_{z,G} = 0 \quad (8)$$

All terms in Eq. 7 as well as $F_{z,I}$ in Eq. 8 are zero. Therefore...

$$F_{z,T} = -F_{z,G} \quad (9)$$

To determine $F_{\rho,I}$, we need to know the direction of the Tensile Force Vector. To determine the direction, we need to know the curvature of a tether that is strung between the section of the ring and an anchor point optimally positioned on the surface of the planet.

978-1-6654-9032-0/23/$31.00 ©2023 IEEE

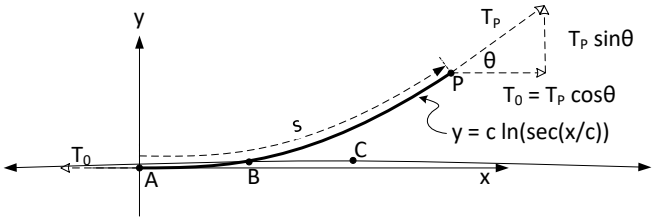

Figure 2: The curve formed by the tether.

To derive the equations that describe the tether curvature, let us assume the following:

1) A constant gravity field,
2) The cross-sectional area of the tether is proportional to the tension within the tether.

In the literature, assumption (2) is referred to as "The Catenary of Equal Strength" [10], "The Constant Stress Catenary" [11], or "The Constant Stress Cable" [12].

Let 's' represent some distance along the tether from point 'A' towards point 'P', where at 'A' the slope of the tether is zero.

Let 'θ' be the angle in radians at Point P,

Let 'T_P' be the tension at Point P,

Let 'T_0' be the tension at Point A,

Let 'σ_{const}' be the constant stress that the tether is designed to be under,

Let 'ρ' be the density of the tether material, and

Let 'g' be the acceleration of gravity.

Equations that define the tether shape (see: [11] page 34 and [12] page 114) are:

$$y = c \ln\left(\frac{1}{\cos\left(\frac{x}{c}\right)}\right) \tag{10}$$

$$x = c \operatorname{acos}\left(e^{-\frac{y}{c}}\right) \tag{11}$$

$$\theta = \frac{x}{c} \tag{12}$$

$$s = c \ln\left(tan\left(\frac{\pi + 2\theta}{4}\right)\right) \tag{13}$$

$$s = c \operatorname{acosh}\left(e^{\frac{y}{c}}\right) \tag{14}$$

$$A_{Cross\_Sectional} = \frac{T_0}{\sigma_{const}} \cosh\left(\frac{s}{c}\right) \tag{15}$$

$$x = 2c \operatorname{atan}\left(e^{\frac{s}{c}}\right) - \frac{c\pi}{2} \tag{16}$$

$$y = c \ln\left(cosh\left(\frac{s}{c}\right)\right) \tag{17}$$

$$T_0 = T_P \cos(\theta) \tag{18}$$

Where:

$$c = \frac{\sigma_{const}}{\rho g} \tag{19}$$

(Note: Equations 13 and 14 will both produce the same result, but 14 may be better for implementation in code.)

These equations describe the shape of the tether when it is acted on by a uniform gravity field, which is an engineering approximation that we will make in this case. To see what the shape of the tether looks like, we can insert some real-world engineering values.

The constant 'c' is calculated by using Eq. 19. Commercially available carbon fiber has a Tensile strength of up to 6370MPa and a density of 1800 kg/m^3 [26]. If we choose carbon fiber for our tether material, use the acceleration of gravity at the surface of the planet, ignore buoyancy, and apply an engineering factor of 2, then 'c' is calculated to be 180,555. A graph of the tether's curve made by using Eq. 10 is shown in Figure 3, below.

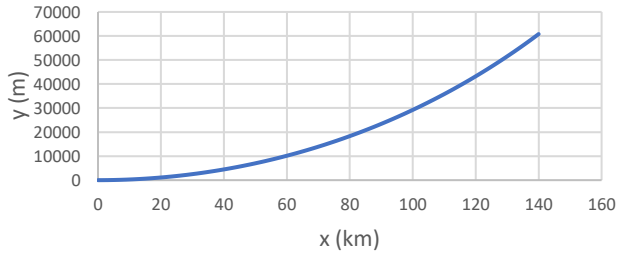

Figure 3: Curve of a carbon fiber tether with an engineering factor of 2.

The change in the cross-sectional area of a tether (neglecting effects associated with forking the tether) is shown in Figure 4 for a tether with an arbitrary thickness of 0.01 m^2 at x=0.

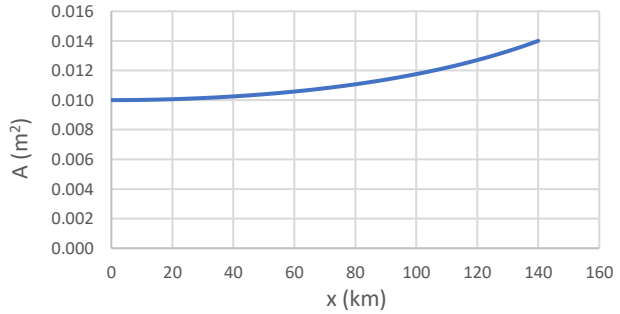

Figure 4: Cross-sectional area for carbon fiber tether w/ engineering factor of 2.

Referring back to Figure 2, above, we will anchor the tether at Point B and attach it to the ring at Point P. A gentle arc, representing the curve of the planet's surface, passes through Points B and C. This arc is positioned so that the center of the arc's circle is directly below Point C. That is, the x-coordinate of the center of the arc's circle is midway between the x-coordinates of Points B and P.

978-1-6654-9032-0/23/$31.00 ©2023 IEEE

The value of the x-coordinate of Point B is an input that is later adjusted iteratively to minimize cost. The y-coordinate of Point B is calculated from its x-coordinate with Eq. 10. The y-coordinate of Point P is the y-coordinate of Point B plus the design altitude of the ring. We can then use Eq. 11 to calculate the x-coordinate of Point P. We now have {x, y} coordinates for Points B and P and we can calculate the direction of the forces (that is, values of θ) at Points B and P by using Eq. 12.

Let's suppose for a moment that we know the value of T. Then we could create force vector components $\{T_x, T_y\}$ for each force by using…

$$T_x = T\cos(\theta) \tag{20}$$

$$T_y = T\sin(\theta) \tag{21}$$

These force vectors are still in a 2D "ground" coordinate system of the planet. We need to perform calculations in the cylindrical coordinate system that we defined earlier for the ring; therefore, we need to rotate these vectors by angles 'ω_B' and 'ω_P'using…

$$\begin{bmatrix} T_x' \\ T_y' \end{bmatrix} = \begin{bmatrix} \cos\omega & -\sin\omega \\ \sin\omega & \cos\omega \end{bmatrix} \begin{bmatrix} T_x \\ T_y \end{bmatrix} \tag{22}$$

Figure 5, below, illustrates the rotation for angle ω_P.

Let us define a unit tensile force vector, $\{T_{Px}, T_{Py}\}$, at Point P. Since the tether, where it is attached at Point P, is pulling down and to the left in Figure 2 (above) we assign 'T_{Px}' to ''$-T_P\cos(\theta_P)$'', and 'T_{Py}' to '$-T_P\sin(\theta_P)$'.

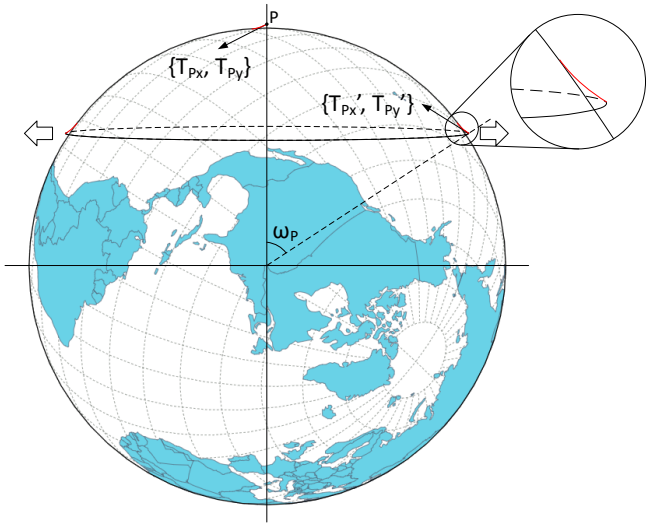

Figure 5: Rotation of the Tensile Force Vector Derived from the Catenary

The angle of rotation, 'ω_P' in degrees, for our rotation formula is

$$\omega_P = -(90^\circ - EqLat) \tag{22}$$

Where:
'$EqLat$' is the "Equivalent Latitude" of the ring, or the latitude the ring would be at if its axis were the same as the axis of rotation of the planetary body.

The rotated vector we obtain for Point P, $\{T_{Px}', T_{Py}'\}$, is now a useful vector within the cylindrical coordinate system of the ring because its direction is now the same as that of the F_T vector used in Eq 4.

Similarly, the angle of rotation, 'ω_B', for our rotation formula is

$$\omega_B = -\left(90^\circ - EqLat - \text{atan}\left(\frac{u}{r_P}\right)\right) \tag{23}$$

Where:
'u' is the distance along the x-axis in Figure 2 (above) from Point B to Point P, and
'r_P' is the radius of the planet.

The rotated vector, $\{T_{Bx}', T_{By}'\}$, is now also a useful vector within the cylindrical coordinate system of the ring.

Different values are used for 'ω_P' and 'ω_B' so that the 2D shape of the tether curve will wrap around the planet and thus conform to the curved surface of the planet. In effect, the shape of the tether is remapped from its original {x, y} cartesian coordinate system to a {θ, r} polar coordinate system. In this step, the uniform gravity field also changes into a radial gravity field.

Since we already know $F_{z,T}$ from Eq. 8, we can use the new vector, $\{T_{Px}', T_{Py}'\}$, to calculate $F_{\rho,T}$ with:

$$\frac{T_{Px}'}{T_{Py}'} = \frac{F_{\rho,T}}{F_{z,T}} \tag{24}$$

If we combine the steps above into a single formula, we get…

$$F_{\rho,T} = F_{z,T}\left(\frac{-T\cos(\theta_P)\cos(\omega_P) + T\sin(\theta_P)\sin(\omega_P)}{-T\cos(\theta_P)\sin(\omega_P) - T\sin(\theta_P)\cos(\omega_P)}\right) \tag{25}$$

Note that the T's in Eq 25 cancel out. Using trigonometric identities, Eq. 19 is further reduced to

$$F_{\rho,T} = \frac{F_{z,T}}{\tan(\theta_P + \omega_P)} \tag{26}$$

Now that we have '$F_{\rho,T}$', we can rearrange Eq. 4 and solve for '$F_{\rho,I}$'

$$F_{\rho,I} = -F_{\rho,T} - F_{\rho,G} \tag{27}$$

From the required forces, it becomes possible to calculate the thickness of the tethers per meter of ring, the total amount of tether material needed, and thus the total cost of the tethers. We can also determine a mass and speed for the moving rings suitable for generating the required inertial force, $F_{\rho,I}$.

978-1-6654-9032-0/23/$31.00 ©2023 IEEE

The volume of the tether per meter of ring can be obtained by integrating Eq. 15 with respect to 's' over the span from point B to point P as depicted in Figure 2

$$V = \int_{s_B}^{s_P} \frac{\mathrm{T}_0}{\sigma_{\mathrm{const}}} \cosh\left(\frac{\mathrm{s}}{\mathrm{c}}\right) ds \tag{28}$$

Integrating…

$$V = \frac{c\,\mathrm{T}_0}{\sigma_{\mathrm{const}}} \left[\sinh\left(\frac{\mathrm{s}}{\mathrm{c}}\right)\right]_{s_B}^{s_P} \tag{29}$$

Tethers are progressively bundled so that there are many attachment points at the ring and relatively few at the ground, to allow room for aircraft and ships to easily navigate between them. Bundling also reduces the tethers' cross-section to the wind at lower altitudes. Close to the ground tethers are, at least partially, unbundled to permit a less congested layout of tether tensioning and maintenance systems installed on tether anchor platforms.

The mass of the tethers is their volume times the density of the tether material, and their cost is the mass times the cost per kg for the tether material.

Primary components of the tethered ring's operating costs include:

- Replacement of energy lost to air friction
- Replacement of energy lost to magnetic friction
- Energy used for active magnetic levitation
- Energy used by station-keeping thrusters
- Upkeep

Later sections cover operating costs for supported systems, such as the transportation system and the launch system.

Energy Losses Due to Moving Ring's Air Friction

The moving rings travel within the stationary rings' evacuated sheaths. No engineered vacuum is perfect in practice; therefore, some momentum exchange occurs as the remaining molecules bounce back and forth between the moving ring and the inner wall of the evacuated sheath. One way to conservatively estimate the power loss due to air friction is to assume that when each molecule in the rarified gas touches a surface, it is accelerated to the speed of that surface so that surface-to-molecule kinetic energy transfer efficiency is 100%. We will also assume that the molecule instantly reaches thermal equilibrium with the surface, and then that it then immediately departs in a random direction.

The root-mean-square (rms) speed, 'v_{rms}', of a free-floating molecule is

$$v_{rms} = \sqrt{\frac{3k_B T}{m}} \cong 493\ m/s \tag{31}$$

Where:
'k_B' is the Boltzmann constant, 1.38×10^{-23}J/K,
'T' is the absolute temperature, for example, 273K,
'm' is the molecule's mass, such as 4.65×10^{-26}kg for N_2

The translational speed (speed across the gap), '$v_{x,rms}$', is one-third of v_{rms}. The molecule's average round-trip time is $2d/v_{x,rms}$ where 'd' is the distance between the two surfaces. Therefore, the round-trip time for the gas molecule is

$$t = \frac{2d}{\frac{v_{rms}}{3}} = \frac{6d}{v_{rms}}$$

If a molecule is accelerated in the y direction from zero to the speed of the moving ring, v_y, when it contacts the moving ring, then its kinetic energy will increase by

$$K = \frac{1}{2}m\left(\left(\sqrt{v_{x,rms}^2 + v_y^2}\right)^2 - v_{x,rms}^2\right) = \frac{1}{2}mv_y^2 \tag{32}$$

Let us assume that the molecule is decelerated in the same way when it contacts the inside wall of the sheath. The rate of energy transfer *for a single molecule* will then be

$$Power = \frac{K}{t} = \frac{1}{2}mv_y^2 \div \frac{6d}{v_{rms}} = \frac{mv_{rms}v_y^2}{12d} \tag{33}$$

Considering a one-meter-long "unit" portion of the ring, the power used by that portion will be

$$Power_{unit} = \frac{mv_{rms}v_y^2}{12d} \cdot N \tag{34}$$

Where 'N' is the number of molecules in the space between the unit portion of the moving ring and its sheath. From the ideal gas law…

$$N = \frac{PV}{k_B T} \tag{35}$$

Plugging this into Eq. 34, we get

$$Power_{unit} = \frac{mv_{rms}v_y^2}{12d} \cdot \frac{PV}{k_B T} \cdot n_{rings} \tag{36}$$

If we solve this equation using the mass, m, of N_2 gas molecules and values from the tethered ring reference design (v_y = 18,224 m/s, d = 0.001, V = 0.000113 m^3, n_{rings} = 5) we find that Eq. 36 simplifies to

$$Power_{perMeter} = 94839 \times P \text{ Watts} \tag{37}$$

Where:
'P' is the gas pressure.

978-1-6654-9032-0/23/$31.00 ©2023 IEEE

For example, at a vacuum level of 10^{-9} torr (1.3332e-7 Pa), the same vacuum level as is maintained within the 4km-long pipes of the LIGO instruments, the power needed to make up for the energy lost due to air friction within 1m sections of all 5 moving rings would be $0.012\ W$. It should also be noted that the lost kinetic energy is converted to heat energy, half of which is absorbed by the moving rings and half of which is absorbed by the stationary rings.

This is an area where further research work could be done to determine, for example, if the interior surfaces can be engineered to reduce the efficiency of surface-to-molecule energy transfer to a value of less than 100%.

Energy Losses Due to Moving Ring's Magnetic Friction

Magnetic fields support (or "confine") the moving rings of the tethered ring. Heritage technologies that use the same techniques include magnetically levitated trains and magnetic bearings. Magnetically levitated trains ride on a linear maglev track, but they are exposed to air friction and must make frequent stops; therefore, extremely low magnetic friction is not needed to make them economically viable. Some applications of rotating magnetic bearings, such as a Flywheel Energy Storage System (FESS), have more stringent requirements in this regard. A modern FESS will typically use a disk of "shrink-wrapped" high-specific strength fibers for the energy storage disk and a steel shaft that is levitated with Permanent Magnet Biased (PM-biased) homopolar Active Magnetic Bearings (AMBs). The rotating disk is housed within a vacuum chamber to minimize air friction.

Changing magnetic fields within a magnetic levitation system will induce eddy currents to flow in any conductive materials that the fields penetrate. Changing fields can also generate hysteresis losses. The use of homopolar AMBs can help to minimize such losses in FESSs.

A homopolar AMB is a bearing wherein the magnets are arranged so that a point on the rotor's surface will only travel past same-polarity magnetic poles (either all North or all South). In a heteropolar AMB, the point will travel past poles of alternating polarity. Therefore, in a homopolar AMB, the rotor material sees less variation in the magnetic field strength as it rotates past the magnetic poles in the stator – but it will still see some variation as the under-pole positions and between-pole positions may have different field strengths. To eliminate magnetic friction more completely in a tethered ring, the moving rings require high magnetic field homogeneity in their direction of travel.

A different heritage technology that pushes the envelope on high magnetic field homogeneity is Magnetic Resonance Imaging (MRI), as MRI equipment generally requires a homogeneity (field uniformity) on the order of a few parts per million (ppm) within the imaging area. Engineers use the process of shimming to achieve high homogeneity. When an MRI magnet is manufactured and installed, some shimming might be done by placing metal shims in appropriate locations. Magnets also contain shim coils and shimming is achieved by adjusting the electrical currents in these coils. Engineers do general shimming when they install or service a magnet. Automated systems do additional shimming for individual patients.

Magnetic fields will be distorted by the magnetic permeability of the various materials that they pass through; therefore, the moving ring must also be engineered and manufactured to be as uniform as possible in its direction of travel (see: "Axially Homogeneous Mass Stream" in Table 1, above) to minimize magnetic field distortion.

In the magnetic confinement system for a moving ring, a magnetic field has a bias component and a control component. Most of the bias component can be generated by using permanent magnets rather than currents in coils to avoid consuming power or generating heat – although the shimming electromagnets, if used, will still consume some power, and generate some heat. The shimming electromagnets' power consumption is defined by the ability of the permanent magnet manufacturing process to both minimize part-to-part field strength variations and make magnets that fit together as seamlessly as possible.

The bias field strength needs to be as consistent as possible in the direction of travel of the moving ring. This is achieved first by uniformly distributing the loads supported by the rings as much as is practical, and second by utilizing additional means of load support. Conceptually speaking, the components of load include the uniformly-distributed-static-loads component and the other-loads components, such as non-uniform static loads, point loads, and dynamic loads. The other-loads component can be further subdivided into "loads supported by the other systems" and remaining loads that leak over to the rings, called "leak-over" loads. Uniformly distributed static loads can be supported by the bias component of the magnetic field, and uniform bias fields will not generate magnetic friction.

The dynamic component of any leak-over loads will tend to perturb the rings. In response, the control component of the magnetic fields will need to change to keep the moving rings centered within their confinement magnets. It is the changes in the control fields that create the conditions needed for magnetic friction to occur.

Magnetic friction minimization is achieved by a) Engineering the moving rings to minimize the degree to which changing magnetic fields result in energy losses, and b) Minimizing how often and how much magnetic field strength needs to change due to leak-over loads.

To minimize the degree to which changing magnetic fields result in energy losses, materials that are magnetically permeable but not electrically conductive, such as ferrites, can be used to minimize eddy currents. These materials are not as strong as metals and thus magnetic bearings tend

978-1-6654-9032-0/23/$31.00 ©2023 IEEE

instead to employ magnetically permeable ferrous steels arranged into lamination stacks to break up eddy current loops. However, the moving rings do not need high mechanical strength; therefore, the use of ferrites in their construction is a cost-performance trade-off worth considering.

A variety of load management techniques can be used to minimize how often and how much magnetic field strength needs to change due to non-uniform loads. It may not be necessary, or cost-effective, to employ all such techniques; however, since these techniques are far less novel than the idea of deploying a set of large magnetically levitated spinning rings, let us consider the possibility of implementing as many load management techniques as possible to make the technical requirements for the moving rings' magnetic levitation system less stringent.

The first technique is the use of a system of stringers and inverted catenaries to distribute a point load uniformly along a long section of the ring. Examples of non-inverted catenaries include the main cables of suspension bridges and the curved wire that supports the level electrical wire(s) over a railway track to power electric trains. This system of catenaries and stringer cables can also serve as a suspension system to help isolate the ring from impulse loads. Computer-controlled active suspension may be able to further improve the degree of mechanical isolation that is achieved.

In Table 2, below, we define a factor

$$f_b = \frac{m_L + m_{CS}}{m_L} \tag{38}$$

Where:
'm_L' is the mass of the load, and
'm_{CS}' is the mass of the catenary cables and stringers

Another technique involves making loading more uniform by pumping fluids, such as water and fuels, through pipes between ballast tanks. Load uniformity can be regulated by "zoning" the ring. For example, a zone above a city might be zoned for supporting elevator cables down to the surface, and a zone between cities might be zoned for supporting solar panels and habitats (see [1] for more information on these concepts). Zoning would help to ensure that the entire ring is uniformly loaded with minimal use of ballast weight. It also implies that the cost per kg supported may be varied in practice so that zones with higher demand subsidize zones with lower demand.

Point loads that are vertical, dynamic, and predictable can be made more uniform in time by using counterbalances and dynamic tensioning systems affixed to the ground. Consider, for example, an elevator system designed to carry people and cargo between the ground and the ring. A funicular system with four bull wheels, two at the top and two at the bottom, would ensure that a load going up was counterbalanced by a load going down. To ensure that cars' static loads are always constant, their payloads could be topped up with low-priority loads (for example, freshwater going up and wastewater coming down) before they depart. On the upward elevator trip, during the acceleration phase, automated systems can remove tension from the bottom of the cable to keep the load at the top of the cable from increasing. During deceleration, those same systems can increase the tension at the bottom of the cable to prevent the load at the top of the cable from decreasing. If the elevator accelerates and decelerates at 'a_e' m/s, then the constant load will be (very roughly)

$$Load_{Cable+Car} = m_{Cable}g + m_{Car}(g + a_e) \tag{39}$$

Where:
'g' is the acceleration of gravity.

In Table 2, below, we will define a factor

$$f_c = \frac{g + a_e}{g} \tag{40}$$

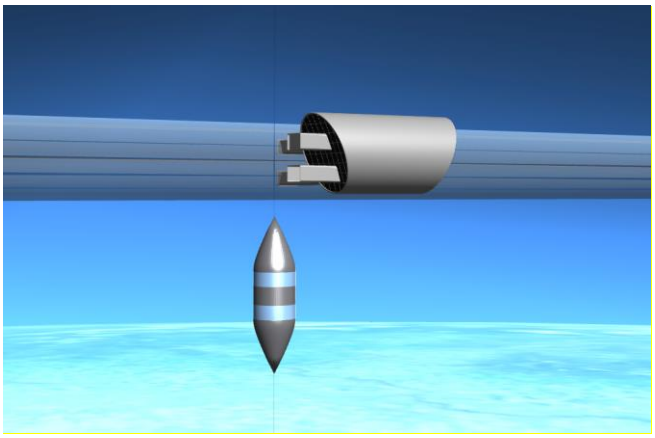

Figure 6: Elevator car approaching upper terminal

Horizontal loads, for example, those generated by accelerating and decelerating transit vehicles, can be transferred between vehicles by adding mass to the rails that the vehicles travel on. In this way, the force of a vehicle accelerating in one direction can be canceled out by the force of accelerating another vehicle in the opposite direction. In Table 2, below, we will define a factor

$$f_d = \frac{gm_R}{F_R} \tag{41}$$

Where:
'm_R' is the amount of extra mass added to the rails, and
'F_R' is the amount of force that the rails can transfer between various accelerating and decelerating vehicles.

The horizontal loads generated by an electromagnetic launch system for spacecraft cannot be transferred between vehicles but can be transferred to the ground through a long stringer-supported cable that connects the end of an electromagnetic mass-driver to an anchor point on the surface hundreds of kilometers downrange of the launcher. However, in the

978-1-6654-9032-0/23/$31.00 ©2023 IEEE

section on space launch, below, the system that we analyze places the mass driver on the surface so that it does not apply horizontal loads to the ring.

As with the elevator cables, tether tension (or tension within any load-bearing cable system) can be dynamically adjusted by using winching systems and actuators. Such adjustments are primarily useful for changing the magnitude, but not the direction, of the tensile force vector; however, there are ways to alter the tether geometry to slightly change the direction of a tether tensile force vector as well.

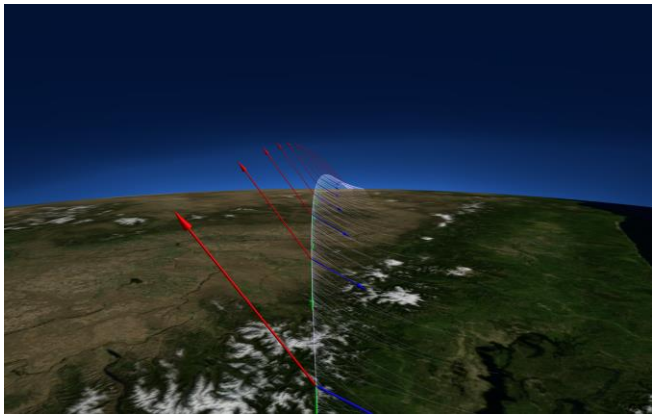

Figure 7: Force arrows from the perspective of someone above the ring looking down

Aeronautic systems may also be employed and represent perhaps the most versatile of the load management solutions. For example, because there will be prevailing winds at the altitude of the ring, the stationary ring should be airfoil-shaped to reduce its coefficient of drag. By simply changing this airfoil's angle of attack, the lift can be increased or decreased which provides a very cheap and responsive means of transferring some load from the ring to the air stream.

A more complex aeronautic system involves thrusters, such as an electrically powered ducted fan or a simple pressure-fed rocket mounted on a gimble. Such systems would be fast-reacting, but also expensive to operate; therefore, they must be reserved for handling only the highest-value dynamic loads, such as those created by transit vehicles and launched spacecraft, as well as sudden, unanticipated dynamic loads.

In Table 2, below, we will define a factor

$$f_e = \frac{g m_{AT}}{F_{AT}} \tag{41}$$

Where:
'g' is the acceleration of gravity at the ring,
'm_{AT}' is the mass of a gimbaled aeronautic thruster, and
'F_{AT}' is the force that the thruster generates.

In Table 2, below, we will also define the value 'x' to be the cost of operating the aeronautic thruster.

Table 2 summarizes the costs associated with supporting loads.

Table 2: Load types and their capital and operating costs

Type of Load	Capital Cost (USD/N)	Operating Cost (USD/N·s)
Uniformly Distributed, Static	a	w
Point Load, Periodic, Static	$b = af_b$	w
Point Load, Vertical, Dynamic but Predictable	$c = bf_c$	w
Point Load, Horizontal, Dynamic but Predictable	$d = af_d$	w
Point Load, Vertical, Static but traveling horizontally	$e = af_e$	z = w + min(x, y)

Where:
'f_b' is a factor for adding stringers and catenary cables,
'f_c' is a factor for adding extra elevator cable tension,
'f_d' is a factor for adding tensile strength to rails,
'f_e' is a factor for adding aeronautical thruster systems,
'w' is the operating cost factor for uniformly distributed loads,
'x' is the cost of operating aeronautic thrusters, and
'y' is the cost of not operating aeronautic thrusters but instead accepting the losses associated with increased leak-over loads.

Code that implements the above math (and which is available on GitHub) currently estimates the value of 'w' to be 120 USD/kg when the ring's altitude is 32km and when the tether's engineering factor is set to 2.

Since 'y' is difficult to estimate without doing more research, let us assume for now that $y \gg x$. With this assumption, $z = w + x$. We can estimate 'x', the cost of operating aeronautic thrusters, by using data from the Ingenuity Mars Helicopter[13] (see Figure 8, below) which was designed to fly in the rarified atmosphere of Mars. Ingenuity draws 350 Watts when flying and generates more than enough thrust to lift itself off the surface of Mars. Its mass is 1.8kg, but on Mars, it weighs 0.7kg; therefore, its propulsion system generates at least 0.7kg×9.8m/s = 6.86N of thrust. If wholesale electric power, $Cost_E$, is 0.05 USD/kWh then we can calculate 'x' to be:

$$x = \frac{Power \cdot Cost_E}{Thrust} \tag{42}$$

Plugging the above values, we get

$$x = \frac{350W \cdot 1s \cdot 0.05 \frac{USD}{kWh}}{6.86N \cdot 3.6e6 \frac{J}{kWh}} \cong 7.1 \times 10^{-7} \frac{USD}{N \cdot s}$$

978-1-6654-9032-0/23/$31.00 ©2023 IEEE

Figure 8: Mars Ingenuity Helicopter

Another way to estimate the cost of aeronautic thrust is to look at the performance of various aircraft. Aircraft consume fuel to generate lift and overcome drag. For example, the H-60R helicopter consumes 1000lbs/hr of JP5 fuel and weighs, on average, 18,500lbs during a full-range mission.

$$x = \frac{1000\frac{lbs}{hr}\cdot\frac{1}{2.2}\frac{kg}{lb}\cdot\frac{1}{3600}\frac{hr}{s}\cdot 0.82\frac{USD}{kg}}{18500lbs\cdot\frac{9.8}{2.2}\frac{N}{lbf}} = 1.256\times10^{-6}\frac{\text{USD}}{\text{N}\cdot\text{s}}$$

The numbers for a 777-300, a large commercial aircraft, are

$$x = \frac{16{,}750\frac{lbs}{hr}\cdot\frac{1}{2.2}\frac{kg}{lb}\cdot\frac{1}{3600}\frac{hr}{s}\cdot 0.82\frac{USD}{kg}}{\frac{(299.37+237.68)}{2}Tons\cdot 9800\frac{N}{Tons}} = 6.59\times10^{-7}\frac{\text{USD}}{\text{N}\cdot\text{s}}$$

While this data is anecdotal, and it only considers the energy costs, it does suggest that an electrically powered high-altitude aeronautic thruster will not only generate thrust sustainably, but it will also, on the USD/(N·s) metric, outperform an aircraft powered with jet fuel.

4. TERRESTRIAL TRANSIT

The state-of-the-art technology for long-distance travel is fossil-fuel-powered aircraft, but the need to transition to a carbon-neutral economy is driving the need for a sustainable alternative. In addition to their passengers and cargo, aircraft must carry fuel, landing gear, wings, tail, and engines. Their airframes are structurally reinforced because they need to take off, climb to altitude, descend, and land safely. Fuel is consumed both to generate lift and to overcome drag. The airports that they take off and land at require a lot of real estate and airplane noise devalues the property near these airports. Passengers must incur security screening delays to prevent aircraft from being hijacked and weaponized by terrorists. Finally, the economics of aircraft favors larger passenger manifests with less frequent departures, which increases travel times and decreases convenience - especially when direct flights are not available.

High-speed electric trains are a suggested alternative to aircraft in a carbon-neutral economy, but the corridors for high-speed trains are expensive either because of tunneling costs, viaduct costs, or the cost of acquiring right-of-way.

If a tethered ring is technically feasible as a load-bearing platform, then a stratospheric evacuated or light-gas-filled tube transit system supported by a tethered ring may also be technically and economically feasible. To reduce the number of possibilities under consideration at the same time, let us assume that the transit tube is filled with hydrogen gas and that the gas has a small positive pressure relative to the outside atmosphere so that it will leak out and blow away in the wind in the event of tube puncture. Let us also assume that, at the air pressure and wind speeds at the altitude of the tube, a hydrogen leak will not sustain a flame. While helium gas is non-flammable and is easier to contain within an envelope, it is also denser and more expensive. If studies show that the fire risk for hydrogen is unacceptable, then a double-walled tube can be engineered and the space between the walls can be filled with helium gas to mitigate the risk of fire.

The tube transport system would have five main parts: ground terminuses, elevators, ring terminuses, transit vehicles, and a tube. The tube is filled with the light gas and it contains the magnetic rails that the vehicles' linear AMBs and linear motor-generators engage with.

Passengers ride elevators from a ground terminus up to a high-altitude ring-supported terminus, then board a transit vehicle that carries them around the ring, and then return to the surface by elevator. There are several advantages to such a system.

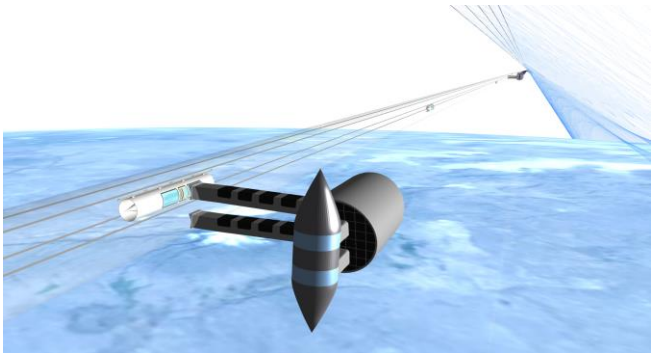

Figure 9: Upper terminus, gas-filled tube, elevator car, and vehicles of a ring-mounted transit system (stringers not shown)

Even in the aggregate, the land needed for ground terminuses would be far less than what is needed for airports. Therefore, many ground terminals can be cited at prime locations within city limits. In the long term, municipalities could reclaim some of the land used by airports and put it to other uses, potentially increasing the value of real estate near the reclaimed airports in the process.

Securing right-of-way and environmental permits for a "stratospheric" tube-transit corridor is easier than for a comparable rail corridor on the ground because, at the altitude of the tethered ring, the tube will be difficult to see from the ground. The high altitude makes it unlikely that the tube will ever be punctured by, for example, a stray gunshot. At the same time, the tube is deep enough within the atmosphere that the probability of it being punctured by a

978-1-6654-9032-0/23/$31.00 ©2023 IEEE

meteor or falling space debris is also minuscule. Even if it were punctured, the outside pressure is 5% of sea-level air pressure, so the hydrogen inside would leak out slowly.

Transit vehicles are lighter than aircraft per passenger because, unlike aircraft, they do not need to carry the additional mass of landing gear, fuel, wings, tail, and engines. Because these vehicles travel within a low-pressure hydrogen-filled tube, less power is needed to overcome aerodynamic drag. These vehicles can travel at subsonic speeds in hydrogen at several times the speed that a subsonic aircraft can travel through air. Because they use magnetic levitation and linear motor-generators for propulsion, power can be recovered through regenerative breaking when they decelerate. Interior cabin noise will be lower than it is in jet-powered aircraft. As each individual vehicle is small, departures are more frequent. With fewer passengers per vehicle, the probability of spreading infections is reduced. As the vehicles travel in a tube and under a maglev track, terrorists cannot hijack and weaponize them; therefore, the efficiency of passenger security screening can be increased. The vehicles will not need a cockpit crew, and fewer cabin crew are needed per passenger mile because the vehicles are faster than subsonic aircraft. Even cabin crew hotel accommodation costs are avoidable because, after an 8-hour shift serving vehicles, a cabin crew will have returned to their starting point and can return home to sleep.

The speed of sound in hydrogen is

$$c = \sqrt{\frac{\gamma \cdot k \cdot T}{m}} = \sqrt{\frac{1.4 \cdot 1.38 \times 10^{23} \frac{J}{^\circ K} \cdot 273.3^\circ K}{3.32 \times 10^{27} kg}} = 1261 \frac{m}{s} = 4540 \frac{km}{hr}$$

Where:
'γ' is the adiabatic index also known as the isentropic expansion factor which is 7/5 for diatomic gases,
'k' is the Boltzmann constant,
'T' is the absolute temperature,
'm' is the mass of a single molecule.

Therefore, a vehicle traveling at 4000km/hr within a low-pressure hydrogen atmosphere would be a subsonic vehicle.

Capital Cost Per Available Seat Kilometer (CASK)

The number of Available Seat Kilometers (ASK) per year for the transit system is

$$n_{ASK} = \frac{n_T n_{PPV} c_{ring} f_{In} v_V n_{spy}}{s_V \cdot 1000 \frac{m}{km}}$$

Where:
'n_T' is the number of express tracks (assuming 2)
's_V' is the spacing of the vehicles (assuming 500m)
'n_{PPV}' is the number of seats per vehicle (assuming 8)
'c_{ring}' is the circumference of the ring
'f_{In}' is an "indirect route" factor of $\sqrt{2}/(\pi/2)$
'v_V' is the vehicle's cruising speed in the express lanes
'n_{spy}' is the number of seconds in a year
'n_{ASK}' is the number of available seat kilometers per year

With the numbers assumed above, n_{ASK} is 14,900 billion km/year. This is enough capacity for every person on Earth to travel the length of mainland Japan once per year. Capacity could be increased further by seating more passengers per vehicle or by reducing the vehicle spacing.

Table 2 can be used to help estimate the cost of the system. The transit tube, even though it is filled with hydrogen, is still a uniformly distributed static load. The ring-mounted terminuses and elevator cables are periodic, static, point loads, and the elevator cars are predictable, dynamic, vertical point loads. Transit vehicles are static vertical loads that travel horizontally, and they generate horizontal, dynamic, and predictable horizontal loads when they accelerate and decelerate.

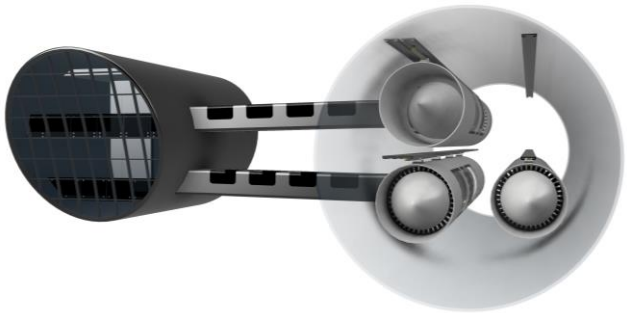

Figure 10: Transit terminus and three transit vehicles

The mass per meter of tube is estimated to be

$$m_{Tube} = 2\pi r t \rho$$

Where:
'r' is the radius of the tube,
't' is the thickness of the tube wall,
'ρ' is the density of the tube wall material.

Using $r = 6m$, $t = 1mm$, and $\rho = 1790$ we get 67kg/m.

The Capital CASK (CCASK) is a metric of critical importance since it has already been established that there are several reasons why the operating costs will be lower for tube transit vehicles than for airplanes. The capital cost per available seat kilometer is

$$CCASK = \frac{(m_{tube} + m_{term}) Cost_{perKg}}{n_{ASK} \cdot Period_{Amortization}}$$

Where:
'm_{tube}' is the mass of the tube and rails,
'm_{term}' is the average mass of the terminuses, elevator cables, cars, etc.

978-1-6654-9032-0/23/$31.00 ©2023 IEEE

Using 67kg/m for m_{tube}, 30kg/m for m_{term}, the reference design's ring circumference of 33,800km, 120USD/kg for $Cost_{perKg}$, the n_{ASK} value we calculated earlier, and a 20-year amortization period, we arrive at a value of 0.00121 USD per ASK. A full breakdown of airline CASK has been published by Saxon[14] which suggests that the total CASK for airlines ranges from 0.0471 to 0.0819 USD/km. This suggests that the capital cost of a tethered ring transit system will not prevent the overall system from being an economically viable alternative to aircraft. A more in-depth analysis of the transit system's CASK is made using code within the tethered ring's digital twin on GitHub[15]. Figure 11 shows cost-breakdown results produced by this code.

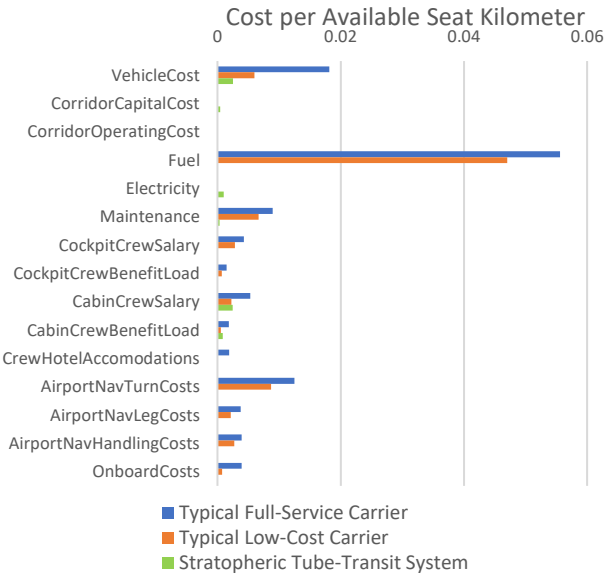

Figure 11: Cost breakdown for full-service and low-cost airlines, and stratospheric tube-transit system

5. SPACE LAUNCH

Many countries have invested heavily in the development of chemical rocket technology for both military and commercial applications. The cost continues to be expensive[1]. Enduring and authoritative sources of truth, including NASA press releases[16], reports from the Office of the Inspector General[17], and the usaspending.gov website[18]–[20], place the current cost of missions to the International Space Station above USD 70,000/kg when using a reusable first stage, disposable second stage, and a reusable capsule.

This section considers two launch system architectures. The first involves mounting the entire length of an electromagnetic launcher, or mass-driver, on the tethered ring at the tethered ring's design altitude. Passengers and cargo would then travel up to the launcher within elevator cars. There they would board a space vehicle which the mass-driver would accelerate down an evacuated launch tube. The vehicle would exit the tube through an airlock with fast-acting doors and travel through the residual atmosphere into space.

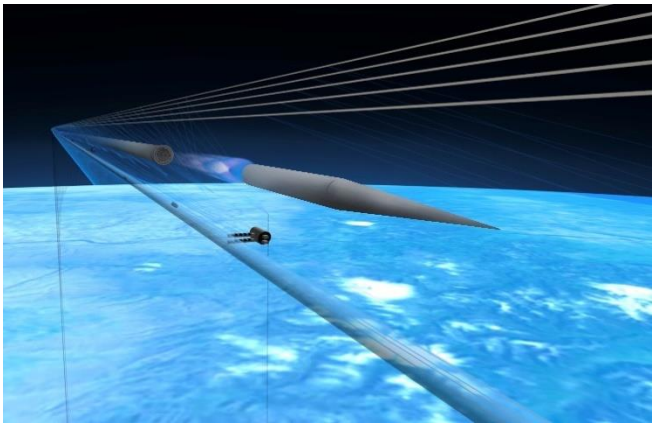

Figure 12: First launch system architecture with a space vehicle exiting the launch tube airlock at high speed.

In the second launch system architecture, the mass driving portion of the launcher is installed slightly below sea level within a concrete pipeline. The vehicle is accelerated within the pipeline to above orbital velocity whereupon it enters, and coasts within, a lighter-weight evacuated tube that is suspended from the tethered ring. It exits the suspended tube at the tethered ring's design altitude and travels through the residual atmosphere into space.

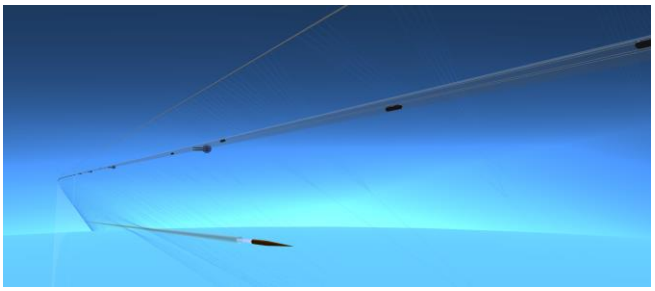

Figure 13: Second launch system architecture with a vehicle exiting a lightweight evacuated tube suspended under the tethered ring.

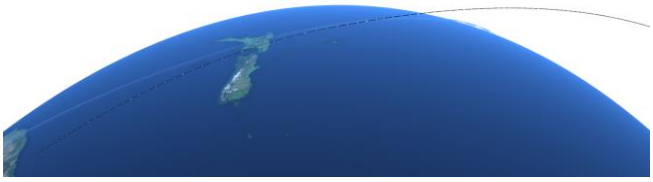

Figure 14: Second launch system's launch trajectory.

Detailed cost analysis in this section is done for the second architecture. The analysis will assume that the launcher is designed to achieve interplanetary launch velocities.

To prevent the vehicle from rapidly decelerating upon entering the rarified atmosphere, when it exits the launch system, a vacuum-optimized rocket engine fires to generate sufficient forward thrust to offset the aerodynamic drag of the atmosphere (see Figure 12). Rocket propellants are circulated through the nose cone to assist with thermal management.

To assess the technical and economic feasibility of these architectures the following costs must be determined:

978-1-6654-9032-0/23/$31.00 ©2023 IEEE

1) The launch system's capital and operating costs,
2) Cost-per-kg to various destinations with the launcher.

To establish these costs, a reference design for the mass driver portion of the launcher is needed. Many different designs have been discussed in the literature, including rail guns, coil guns, space guns, electromagnetic catapults, and Verne guns; however, mathematical analysis of these systems is not straightforward. Our goal here is to describe a reference system that is easy for people with ordinary skills in the art of physics and engineering to characterize and validate.

Let's assume that the launcher needs to be human-rated and capable of putting vehicles on trajectories for the Moon, Mars, Venus, and other destinations within the asteroid belt; therefore, it must support a muzzle velocity, 'v', of around 15km/s and a maximum acceleration, 'a', of 30m/s^2 (about 3 times the force of gravity). The launcher's acceleration length, 'l', will then need to be

$$l = \frac{v^2}{2a} = \frac{\left(15000\frac{m}{s}\right)^2}{2 \cdot 30\frac{m}{s^2}} = 3{,}750{,}000\ m$$

The acceleration time will be

$$t = \frac{v}{a} = \frac{15000\frac{m}{s}}{30\frac{m}{s^2}} = 500s = 8.33\ minutes$$

Let us assume that the launcher is enclosed within an evacuated tube, and the vehicles are supported within the tube by using magnetic levitation.

To accelerate the vehicles, two long, counterrotating, variable-pitch screws (see Figure 15) are installed within the tube (see Figure 16). The screws are balanced so that they can rotate at a high speed. Let us assume the screws are rotated at a constant rate, 'ω', of 200 revolutions-per-second (RPS) by internal electric motors.

Figure 15: Example of a variable pitch screw[21]**.**

The teeth of the screw are constructed from a ferromagnetic material so that the vehicle can couple electromagnetically to the teeth by using linear active magnetic bearing technology.

The pitch of the screws' teeth is the finest near the beginning of the launcher and becomes progressively coarser towards the exit. While the counterrotating screws rotate at a constant rate of rotation, the screws' teeth will accelerate down the length of the screw at a constant rate of acceleration. As the vehicle is magnetically coupled to the teeth, it too will accelerate down the launch tube at a constant rate of acceleration.

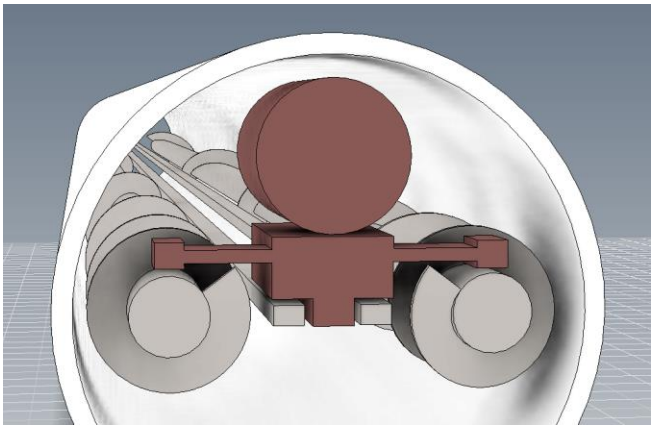

Figure 16: Launch sled with payload (red) magnetically levitated above rails and magnetically coupled to twin counterrotating variable pitch screws (gray) within a tube (white).

The relationship between the rim speed of the screw and the speed of the vehicle is defined by the pitch of the teeth. If the radius of the screw is 0.5m then the teeth are traveling around the shaft at

$$v = 2\pi r\omega = 2 \cdot 3.1415 \cdot 0.5m \cdot 200\frac{1}{s} \cong 628\frac{m}{s}$$

If the goal is for the vehicle to exit the launcher at 15,000m/s, then the slope, or pitch, of the teeth at the launcher's exit must be

$$pitch = \frac{15000\frac{m}{s}}{628\frac{m}{s}} = 23.9$$

If the sled and the loaded vehicle weigh 10 metric tons, then accelerating it at 30m/s requires a forward force, '$F_{\rightarrow}$', of

$$F_{\rightarrow} = ma = 10000kg \cdot 30\frac{m}{s} = 0.3MN$$

If we factor in the mechanical leverage created by the pitch of the teeth then, near the launcher's exit, the sideways force on each of the screw's teeth is

$$F_{\perp} = \frac{F_{\rightarrow} \cdot pitch}{2} = \frac{0.3 \cdot 23.9}{2} = 3.58MN$$

Where:
'$F_{\perp}$' is the sideways force acting on the screws' teeth.

Note that we divide by two here because two screws are

978-1-6654-9032-0/23/$31.00 ©2023 IEEE

accelerating the vehicle.

Since, near the exit of the launcher, the teeth on each screw are pulling predominantly sideways on the vehicle, we need to determine whether it is possible to design a lightweight chassis for the vehicle that can handle these forces in tension. Let us calculate the diameter of a single carbon fiber strut that could support this force without breaking.

$$CrossSectionalArea = \frac{F}{\sigma_T} = \frac{3.58MN}{3.5GPa} = 0.001m^2$$

Where:
'σ_T' is the yield stress under tension.

To convert the cross-sectional area into diameter we rearrange

$$A = \pi\left(\frac{d}{2}\right)^2$$

$$d = 2\sqrt{A/\pi} = 2\sqrt{0.001m^2/\pi} \cong 0.036m$$

Because a single strut with a diameter of 3.6cm can handle these forces, we can conclude that it should be possible to engineer the chassis of a lightweight launch sled to likewise handle these forces.

Next, let us consider whether it is possible to design electromagnets for the linear AMBs that can generate the needed attractive forces.

In an electromagnet, the force exerted, 'F', is related to the energy, 'W_a', stored in the two airgaps between the electromagnet and the plate that is attracting (note: "airgap" is a term used in the art, but technically it is a "vacuum gap" in this application).

$$W_a = \frac{1}{2}B_a H_a 2A_a s$$

Where:
'B_a' is the flux density in the airgaps,
'H_a' is the magnetic field in the airgaps,
'A_a' is the cross-sectional area of each airgap, and
's' is the distance across the airgaps.

In Figure 17, A_a is $length_a \cdot width_a$. If we assume that s is small in relation to A_a, then for small displacements, ds, the magnetic flux, B_aA_a, remains constant. Then

$$F = \frac{dW_a}{ds} = B_a H_a A_a$$

Because 'B' and 'H' are related by

$$\boldsymbol{B} = \mu_0\mu_{r,H}\boldsymbol{H}$$

we can substitute for H_a to get

$$F = \frac{B_a^2 A_a}{\mu_0\mu_{r,H_a}}$$

Where:
'μ_0' is the vacuum magnetic permeability ($4\pi \times 10^{-7}$H/m),
'μ_{r,H_a}' is the relative permeability of the vacuum in the airgap to μ_0 which is 1.

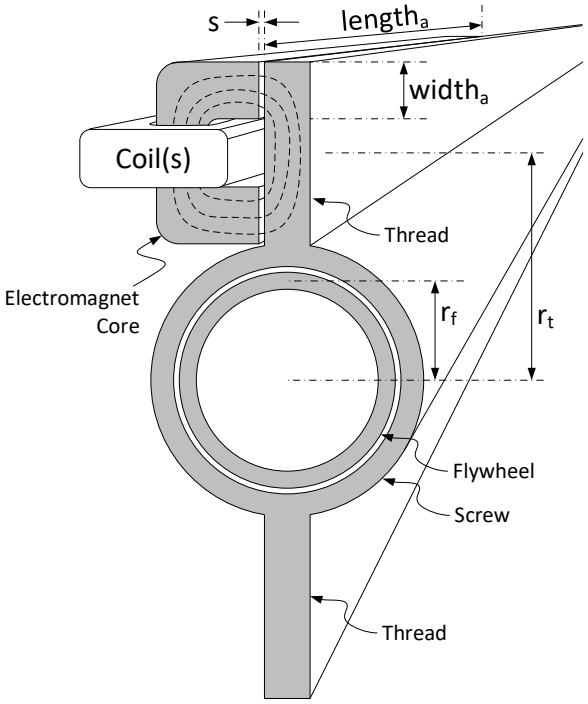

Figure 17: Cross-section of the linear AMB electromagnet coupling to a tooth of a variable pitch screw.

We can assume that the electromagnet will be operated at a percentage, for example, 80%, of its core material's saturation flux density. If we assume a saturation flux density of 1.25T, then the magnetic flux density across the air gap will be $0.8 \cdot 1.25T = 1T$. We now have the information needed to determine the surface area of each screw's teeth that must be acted on (or attracted by) the electromagnets.

$$A_a = \frac{F_\perp \mu_0}{B_a^2} = \frac{3.58MN \cdot 4\pi \times 10^{-7}\frac{\mathrm{H}}{\mathrm{m}}}{(1T)^2} = 4.5m^2$$

If we assume that $width_a$ of the electromagnet is 0.125m, then the length of each magnet will need to be

$$length_a = \frac{A_a}{width_a} = \frac{4.5m^2}{0.125m} = 36m$$

At these dimensions, the weight of AMBs made with traditional copper coil electromagnets would exceed the mass budget for the sled; therefore, lighter weight and more powerful magnetic coupling technology will be needed to reduce the length and weight of the launch sled. This is an area where more work still needs to be done to explore the

978-1-6654-9032-0/23/$31.00 ©2023 IEEE

available engineering options. For example, a technology that employs high-temperature superconductors may be able to satisfy the engineering requirements. Superconductors require cryogenic cooling systems, but the use of cryogenic fuels for rockets and spacecraft is already well-established. It should be noted that another option may be to use cryogen-free superconducting magnet systems, products sold by multiple vendors[22], [23][24].

At the leading and trailing edges of the liner AMBs, there will be changing magnetic fields. To minimize the degree to which these changing magnetic fields result in energy losses, ferrites or lamination stacks (as discussed earlier) can be used where the magnetic fields penetrate the screws' threads. The magnetic field distribution in the air gap can be contoured lengthwise so that changes in magnetic field strength due to the passage of the sled occur more gradually.

The rotational rate of the screws must be maintained as the vehicle is launched. If the vehicle is 36m in length, and it is traveling at 15km/s at the end of the tube, then, when the vehicle is near the launcher's exit, it will apply force to any given position along the threads for only

$$t = \frac{36m}{15000\frac{m}{s}} = 2.4ms$$

The sideways force (which peaks at $F_{\perp} = 3.58MN$ when the sled is near the end of the launcher) must be countered with an opposing force only where and when the vehicle is alongside the screws. The opposing force is generated by rapidly decelerating spinning flywheels housed within the screws. Let's assume that the mass of the flywheels is concentrated in the flywheels' rims. Let's assume that the radius of the flywheel, r_f, is 0.225m. If the sled is 36m in length, and its contact region with each screws' thread is also 36m in length, and if there are 679kgs of flywheel mass per meter of screw, then $36m \times 679kg = 24429kg$ of flywheel mass on each side of the vehicle can be undergoing rapid deceleration to apply the needed force. Decelerating at

$$a = \frac{F_{\perp}}{m} \cdot \frac{r_t}{r_f} = \frac{3.58MN}{24429kg} \cdot \frac{0.5}{0.225} = 326\frac{m}{s^2}$$

would then generate the amount of force (note: $F = ma$) needed to oppose the force that the sled applies to the screw's threads. The change in rim speed due to the deceleration of the flywheels can be expressed as

$$v_f - v_0 = -at$$

Where:
'v_0' is the initial relative flywheel rim speed,
'v_f' is the final relative flywheel rim speed
'a' is the deceleration, and
't' is the deceleration time.

From this, we can calculate that the flywheels need an initial rim speed, relative to the screws, of

$$v_0 = at + v_f = 326\frac{m}{s^2} \cdot 0.0024s + 0 = 0.78\frac{m}{s}$$

Because the flywheels are operating inside the rotating screws, they have an initial absolute rim speed of 283.52m/s. They decelerate to 282.74m/s as the vehicle passes by. The flywheel's rotational rate is initially $200.55s^{-1}$ and is $200s^{-1}$ after the vehicle has passed by.

The flywheels are connected to a torque converter that is designed to decelerate them in the correct amount of time. A set of pawls driven to engage a ratchet by means of electromagnetic actuators connects each flywheel to its torque converter. Magnetic fluids in the torque convertor are electrified to precisely control the amount of torque applied by flywheel deceleration. Between launches, the pawls are retracted, and a small electric motor accelerates the flywheels back up to the correct relative rim speed for the next launch.

Because the thread pitch varies along the length of the launcher, the launcher's linear AMBs are made up of discrete segments that are individually mounted on actuators that are designed to, in a coordinated manner, engage the segments with whatever part of the screw's teeth they happen to be alongside. The actuators can detach and reattach AMB segments as necessary to adapt to the changing geometry of the screw teeth as the vehicle advances down the launch tube.

This conceptually simple launcher design builds upon heritage technologies such as electric motors, flywheels, and linear active magnetic bearings that employ superconducting magnets. Rotating active magnetic bearings that make use of superconductors have been described in the literature[25]–[27].

The design serves to illustrate that there is at least one technically and economically feasible way to launch vehicles from earth to orbital velocities that is not subject to the limitations of the rocket equation. This design was chosen specifically because it should be easy for people with a general knowledge of engineering and physics to independently validate it. Rail guns and coil guns, on the other hand, make use of capacitors and pulsed power equipment, thus more specialized knowledge is needed to analyze the technical and economic viability of these approaches.

Because the dual counterrotating variable pitch screw system uses fast-moving parts, and because such parts come with additional engineering challenges, it would, of course, be preferable to find a way to generate similar kinds of propulsive magnetic fields with fewer moving parts, or ideally, with no moving parts - but without compromising the technical or economic feasibility of the overall system.

Cost Calculation for Electromagnetic Launch

The capital cost of the launcher is a function of both the cost of its components and the loads that it applies to the tethered ring. As was discussed earlier, additional loads increase the capital and operating costs of the ring. The operating cost of

978-1-6654-9032-0/23/$31.00 ©2023 IEEE

the launcher is thus a function of the cost of the electricity that powers the launcher's motors, the portion of the tethered ring's operating costs that are attributed to the dynamic loads from the launcher, and the cost of propellants for the vehicle.

If a vehicle is sent on a mission within the cis-lunar system, we will assume that it will return to earth and be reused. It is possible that vehicles could return to a ring-mounted deceleration system designed to convert some of their kinetic energy back into electricity, reducing the thermal load on the reentering vehicles' thermal protection system in the process. However, we will not cover the cost of vehicle recovery and refurbishment here.

If the vehicle is sent on an interplanetary mission, such as to Mars, then we will assume that the vehicle's cost is largely driven by the need for it to be able to land safely and potentially take off again to return to the Earth.

The cost of the electricity needed to operate the launcher per kilogram of payload launched is simply

$$Cost = \frac{\frac{1}{2} m_{Total} v^2 \cdot Cost_{Electricity}}{m_{Payload} \cdot \varepsilon}$$

Where:
'm_{Total}' is the total sled/vehicle/propellant/payload mass,
'$m_{Payload}$' is the payload mass,
'v' is the launcher exit velocity,
'ε' is the efficiency of the launch system, and
'$Cost_{Electricity}$' is the cost of electricity in USD/GJ

Let us assume an electric motor efficiency of 80% and a wholesale electricity price of 14 USD/GJ. To reach a speed of 15km/s for interplanetary missions, the energy cost will be

$$Cost_{Energy} = \frac{\frac{1}{2} 10tons \left(15000 \frac{m}{s}\right)^2 \cdot 14 \frac{USD}{GJ}}{7tons \cdot 0.8} \cong 2.19 \frac{USD}{kg}$$

The mass of the payload is estimated to be 7 metric tons largely because the vehicle fires its rocket engine to compensate for aerodynamic drag as it exits the atmosphere, and this burn consumes propellants. Therefore, we need to also consider the cost of fuel.

Recall that the launcher in the second launch system architecture is at (or just below) sea level and that the tethered ring supports a suspended evacuated tube that the vehicle coasts within until it reaches the design altitude of the tethered ring (let us assume that is 32km). This tube does not experience any significant dynamic load from the vehicles traveling through it because upon exiting the mass driving portion of the launcher the vehicles are on a hyperbolic trajectory that takes them away from the Earth.

The vehicles exit the suspended evacuated tube through an airlock with fast doors. Let us assume that the vehicle has a long narrow nosecone, like NASA's X-59 (see Figure 18) or NASA's X-43A (see Figure 19), to minimize drag and that it uses transpiration cooling to keep the tip of the nose from melting. The coefficient of drag for the vehicle at 15 km/s is estimated to be 0.05.

Figure 18: The long narrow nosecone of NASA's X-59.

Figure 19: The long flat nose of NASA's X-43A

Figure 20 is a chart of data generated by code[15] that implements the formulas in this paper. It shows us that the vehicle's engine needs to fire for about 20 seconds to prevent the vehicle from decelerating due to aerodynamic drag. During this burn, it consumes 2600kg of propellants. The analysis assumes a hydrolox-powered engine with exhaust velocity equivalent to the Space Shuttle's main engines, the RS-25's. The analysis also assumes that an additional 400kg of the vehicle is classified as non-payload mass (that is, this mass will not be used for landing or otherwise repurposed at the destination). This brings the total non-payload mass to 3 metric tons.

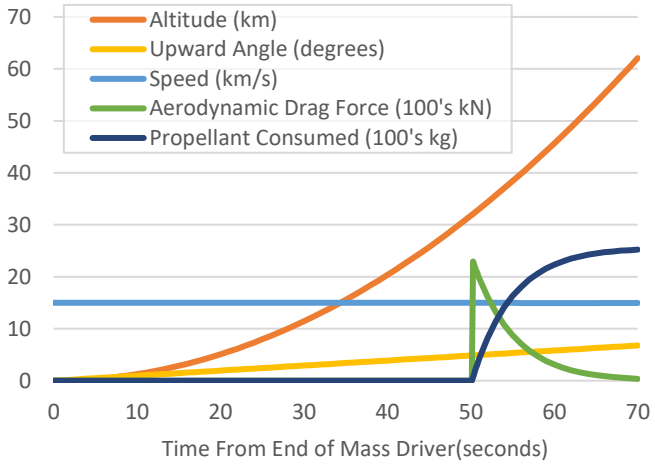

Figure 20: Altitude, upward angle, speed, drag force, and propellant consumed for a 15km/s launch from sea level.

Propellant costs are estimated to be 0.20 USD/kg for LO2 and 3.65 USD/kg for green hydrogen (LH2). After accounting for the stoichiometric ratio of these propellants, the propellant cost is 0.70 USD per kg of propellant or 0.26 USD per kg of payload mass.

978-1-6654-9032-0/23/$31.00 ©2023 IEEE

Table 3: Launch system operating costs per kilogram of payload for interplanetary missions

Launch Velocity	Electricity (USD/kg)	Propellant (USD/kg)	Total (USD/kg)
15 m/s	2.19	0.26	2.45

Table 4 tabulates the values that were used to estimate the capital cost of the launcher.

Table 4: Launcher Capital Cost Components

Parameter	**Value**	**Units**
FlywheelMassPerMeter	679	kg/m
UnderwaterTubeJacketThickness	0.002	m
BracketsMassPerMeter	40	kg/m
RailsMassPerMeter	100	kg/m
ScrewsMassPerMeter	100	kg/m
TorqueConvertorsMassPerMeter	100	kg/m
MotorCost	2000	USD
MotorsPerMeter	0.02	
VacuumPumpCost	2000	USD
VacuumPumpsPerMeter	0.02	
SuspendedTubeMassPerMeter	100	kg/m
UnderwaterTubeInnerRadius	4	m
UnderwaterTubeOuterRadius	4.5	m
Length	3750000	m
AccelerationTime	500	s
SuspendedTubeLength	751527	m
EnergyCostPerKilogram	2.42	USD/kg
TotalCostPerKilogram	2.55	USD/kg
SteelCost	0.89	B USD
MotorsCost	0.15	B USD
VacuumPumpsCost	0.15	B USD
UnderwaterTubeCost	2.69	B USD
SuspendedTubeCost	9.17	B USD
FactoryCost	2	B USD
TotalCost	**15**	**B USD**

The suspended tube represents about 2/3rds of the total system cost. This cost could be reduced if a ramp were placed between the end of the mass driver and the beginning of the suspended tube. The ramp would deflect the launched vehicle upwards slightly and decrease the distance that the vehicle would need to travel within the suspended tube, thus making the tube shorter and reducing its cost.

To arrive at a per-kg cost, the capital cost of the launch system needs to be amortized over some estimate of the total amount of mass that it will launch over its lifetime. A reference mission was described in a prior work[1] that involved sending 1.5 million metric tons to the Moon and Mars. If we use the 1.5 million metric tons number for our amortization of the launcher's capital costs, then

$$Cost_{CapitalAmortized} = \frac{(15\ Billion\ USD)}{1.5 \times 10^9 kg} = 10\frac{USD}{kg}$$

The total cost-per-kg would then be 12.45 USD/kg for the first 1.5 million tons, and then 2.45 USD/kg from there on.

There are additional advantages to adopting an infrastructure-based approach for interplanetary missions.

Launch infrastructure is sustainable. It primarily uses electricity for propulsion, which can be generated renewably. The vehicle's rocket engines, which are used briefly to offset air friction, are fueled with green hydrogen. Green hydrogen does not add CO2 to the atmosphere when it is burned, and it is produced with renewable energy.

Launch infrastructure will reduce the number of rockets that the human civilization needs to launch as part of, for example, an interplanetary colonization effort. When many organizations are building and launching rockets, it becomes more difficult to regulate rocket technology and to prevent it from being disseminated to all corners of the globe. Increasing the prevalence and variety of rocket launches will make it more difficult for the nations of the world to distinguish between the peaceful use of a rocket and a rocket launch that represents an imminent military threat. This could decrease geopolitical stability and increase the cost of implementing threat detection systems for national defense.

Further Work

More engineering work is needed on subjects such as the cost and feasibility of the launch vehicle's thermal protection system, as much of the data on this technology is classified. The rate of heat dissipation from the launcher's screws needs to be analyzed before reasonable estimates of launch rates can be made. Further investigation into lightweight magnetic coupling technologies is needed. Many of the numbers estimated in this preliminary analysis could benefit from refinement.

As was mentioned earlier, an architecturally accurate digital twin of the tethered ring and the systems that it supports is available on GitHub[15]. The digital twin implements the analytical techniques described in this paper, but a more detailed analysis, using special-purpose commercially available software tools, would certainly help to improve the accuracy of its findings.

6. GEOPOLITICAL CONSIDERATIONS

Ideally, a tethered ring should be constructed in the ocean so that it can be as level as possible when it is started up. However, conceivably the ring could be started up while on land if the land is sufficiently flat or if the ring can be made sufficiently circular, despite an uneven landscape, by some other means.

Possible construction locations include the South Pacific Ocean (see Figure 21), and around Antarctica and Australia (see Figure 22). From either of these locations, the ring could be moved anywhere around the world after it has been raised. The best final locations would maximize the number of population centers that the ring's tube transit system can serve. However, if the geopolitical issues prove to be insurmountable, it is theoretically possible, although

978-1-6654-9032-0/23/$31.00 ©2023 IEEE

potentially more challenging, for some nations to build a tethered ring so that it only passes over their own county's territory and international waters (see Figure 23, Figure 24, and Figure 25).

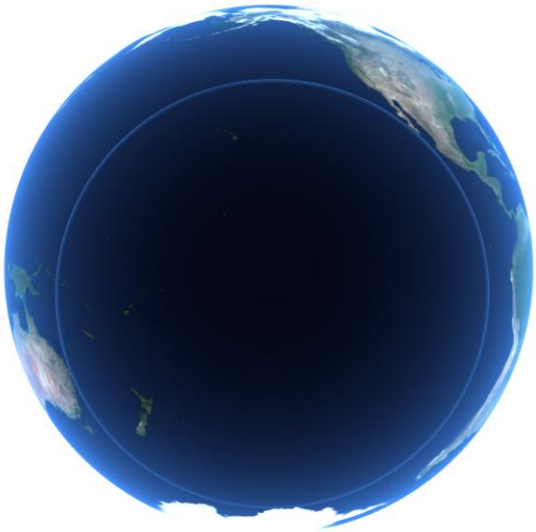

Figure 21: South Pacific Construction Location

Figure 22: Australia, South Africa construction location

Figure 23: Ring placement over Russia and Antarctica

Figure 24: Ring placement over only the United States

Figure 25: Ring placement over only Mexico

978-1-6654-9032-0/23/$31.00 ©2023 IEEE

Resilience to Terrorist Attack

While there is no shortage of ways for a determined team of terrorists to inflict considerable harm on society, it is still worth considering how vulnerable a tethered ring is to terrorism, and what can be done to protect it. Terrorists are more likely to be drawn to a target if they perceive it as an opportunity to inflict a considerable amount of damage with relatively little effort.

The most vulnerable component of an inertially supported active structure is its mass-stream or mass-streams. In the tethered ring, these are the high-speed precision-guided, and magnetically confined moving rings contained within the stationary rings.

The high altitude of the main rings puts them out of reach of aircraft. If a terrorist were to smuggle a bomb onto the transit system and set it off, the main rings would be far enough away from the explosion to not be damaged. The atmosphere at the altitude of the ring is very thin. These conditions are not ideal for propagating an overpressure wave, which makes planning an attack difficult. There is no easy way for a terrorist to get closer to the main rings since there is no way to go outside. In any event, anyone boarding an elevator up to the ring would pass through security screening adequate to ensure that they are not carrying a sniper rifle, large quantities of a high explosive, a portable guided missile, a rocket-propelled grenade, a similar military-grade weapon, or a space suit.

While it is difficult to imagine how someone could set off a high explosive beside one of the main rings, what would happen if they did? The main rings travel at 18223 m/s. The speed at which material from a bomb will expand outwards is much slower, so a bomb would damage the stationary ring, but a moving ring would perceive the explosion as a "glancing blow" and thus would likely escape damage. Thus, the problem of engineering the moving ring to survive the nearby detonation of a high explosive might be solvable. It might also be possible to design the stationary ring in a way that prevents the propagation of damage in the direction of travel of the moving ring.

The tethered ring reference design has five main rings, so if one were to fail, the remaining four would still be able to support the load. The aeronautic stabilization systems may be leveraged to make sure that the remaining four rings do not settle to a new equilibrium too quickly. Engineers must ensure that a damaged ring will break apart and that its fast-moving pieces will either burn up in the atmosphere or fly off into space.

Unlike the precision-guided mass streams, the tethers are strong and thus more resilient to an attack. A direct hit with a high-explosive charge would be needed to sever a thick carbon fiber cable. However, tethers are also attached to the ground which makes them more accessible to terrorists. Engineering the tethers to survive terrorist attacks is a cost issue. The cheapest possible tethered ring design would fail if one tether were to be severed. By adding redundancy and cost, a tethered ring can be designed to remain intact even if some tethers are severed or otherwise fail. If we assume that an attack from ground level is more likely than an attack from the air, then extra redundancy can be concentrated near the anchors. For example, the tethers can be designed to fork as they approach the anchors like the roots of a banyan tree. To succeed, a ground attack would then need to sever all the individual root cables.

Many of the tether anchors will be far offshore and will resemble offshore wind turbine platforms. There is no reason for any unauthorized vessel to approach one, so it should be straightforward to enforce keep-out zones around the anchors and defend them by attacking any unauthorized vessels that come too close. Onshore tether anchors will need to be set up within security perimeters. The real estate within these security perimeters does not need to be repurposed; it just needs to be made more secure to deny potential terrorists direct access to the tether roots.

At higher altitudes, the tether will be out of range of a terrorist armed with, for example, a rocket-propelled grenade. A terrorist would then need an aircraft or a helicopter to attack the tether. As aircraft are more difficult for terrorists to acquire, less redundancy and lower cost may be considered acceptable for higher altitude sections of the tethers.

Since the tethers are aeronautically stabilized, the thruster nacelles can be employed to push a tether sideways as needed to get out of the way of an approaching aircraft. A tether could also be designed to deploy an airbag that would help it survive the initial contact with the plane. Then the plane would simply be knocked out of the sky by the tether, like a dragonfly colliding with the string of an archer's bow. The tether's tension could be reduced if it detected that a collision with an airplane was imminent, which would increase the chances of the tether surviving the collision.

There is a lot more that can be written on this subject, but the main point is that, upon closer examination, a properly engineered and secured tethered ring is not an easy terrorist target. The primary reasons for this are that: a) The mass stream's high altitude and separation from the transit system makes it difficult for terrorists to access, b) the mass stream's circuit never takes it close to the surface, and c) with multiple redundant mass streams, tethers, and tether roots, the architecture does not have any single point of failure that terrorists could exploit.

The Disaster Scenario

If despite our best engineering efforts, containment of all the tethered ring's mass streams was to be lost, the considerable kinetic energy of the moving rings would be released into the upper atmosphere. Possibly the rings would burn up in the upper atmosphere and possibly they would be moving fast enough to escape the Earth's gravity well. If all the energy

978-1-6654-9032-0/23/$31.00 ©2023 IEEE

were to be released into the upper atmosphere, it would be roughly equivalent to the amount of energy that a hurricane releases in about 5 minutes. However, it takes 30 minutes for the rings to complete one revolution. If we imagine all the energy being released in one location, then it would be released over a period of 30 minutes. However, it would be easy enough to scuttle the entire ring if, for example, damage occurred over a population center, so that the energy release would be evenly distributed around the entire ring's circumference rather than concentrated in one location.

Without the moving rings, the rest of the structure would fall back towards earth at the "terminal velocity" of the ring. All parts of a tethered ring (that is, the transit tube, habitats, and main rings) are lightweight in proportion to their cross-sectional area; therefore, their terminal velocity will not be high. The main rings are outfitted with solar panels which can be angled like wings to guide and help slow their fall. The tethered ring and its tethers are also outfitted with thruster nacelles for aeronautic stabilization and supporting dynamic loads. These can be used to guide the ring to a predetermined landing zone on the earth, and to decelerate the components from terminal velocity to zero as they approach the surface. It is unlikely that the weight of a tethered ring would crush any buildings or vehicles that it landed on, and the landing zone can be zoned for "no fragile structures" in the same way the building code in some cities requires buildings to be made earthquake-proofing. The landing zone may be outfitted with loud alarms to warn any people and animals that happen to be in the zone and directly underneath a falling ring to clear out of the way.

The tethered ring's habitats and transit vehicles will need to be designed to keep people alive while they are floating in the ocean – at least long enough to permit emergency responders to rescue the people inside. As these systems are already designed to keep people alive near the edge of space, this requirement will likely not present an insurmountable engineering challenge.

While the tethered rings' redundant systems make such a scenario unlikely, it will be reassuring to know that the tethered ring is engineered to fall back to earth in a way that causes a minimal amount of property damage and loss of life.

7. CONCLUSIONS

The tethered ring is an inertially supported active structure that employs a constant length, constant gravitational potential, and constant lateral acceleration mass stream to achieve low magnetic friction and thus low operating costs. The hydrogen-filled tube transportation system permits vehicles to travel at speeds of 4000 km/hr without exceeding the speed of sound in the low-pressure hydrogen atmosphere. It provides a way to transition the long-haul transportation industry away from airliners and over to a fully carbon-neutral technology that is faster, more convenient, and has lower operating costs. The capital cost of the system was estimated to be 0.00121 USD per ASK (Available Seat Kilometer).

A launch system is also described for launching mass to the moon, other nearby planets, and the asteroid belt that achieves an estimated levelized per-kilogram launch cost of 12.45 USD/kg when the system's capital costs are amortized over 1.5 million metric tons of payload. To improve geopolitical viability, several options are presented where tethered rings can be constructed in one place and then relocated to another place. The subject of the architecture's resilience to terrorism is discussed as well as the failure scenario, should an attack be successful or should an unforeseen accident occur.

8. ACKNOWLEDGEMENTS

The author would like to thank Alastair Swan and Ceana Prado Nickle for their ongoing years of support in developing the technology, and of course, for their latest contributions as reviewers of this paper. The author also thanks Troy Moss for his modelling work used in Figure 9 and 10, Justin Siples for his work on modelling the transit vehicles depicted in Figure 10, Alice Dowling for her work on Figure 12, and Alex de Marne for the 3D model shown in Figure 16.

9. REFERENCES

[1] P. Swan, "Electromagnetic Space Launch Infrastructure – A Techno-Economic Analysis," *2022 International Conference on Electromagnetics in Advanced Applications (ICEAA)*, pp. 400–405, Sep. 2022, doi: 10.1109/ICEAA49419.2022.9900032. Available: https://www.project-atlantis.com/wp-content/uploads/2022/09/ICEAA_APWC_2022_FullLengthPaper_Swan_2022_09_08.pdf

[2] P. L. Swan, "Elevated load-bearing platform," 11,014,692 B2, Aug. 21, 2015 Accessed: Oct. 08, 2022. [Online]. Available: https://www.project-atlantis.com/wp-content/uploads/2021/ElevatedLoadBearingPlatform_PhilipSwan_FromUSPTOWebsite.pdf

[3] G. Schweitzer and E. H. Maslen, "Magnetic bearings: Theory, design, and application to rotating machinery," *Magnetic Bearings: Theory, Design, and Application to Rotating Machinery*, pp. 1–535, 2009, doi: 10.1007/978-3-642-00497-1/COVER.

[4] A. Yunitskiy, "'в космос на колесе' ('To Space by Wheel')," *Техника-молодежи ("Technical Youth")*, no. 6, pp. 34–37, Jun. 1982, Accessed: Oct. 08, 2022. [Online]. Available: http://zhurnalko.net/=nauka-i-tehnika/tehnika-molodezhi/1982-06

[5] P. Birch, "Orbital Ring Systems and Jacob's Ladders - I," *J Br Interplanet Soc*, vol. 35, pp. 475–497, 1982, Accessed: Oct. 08, 2022. [Online]. Available: http://buildengineer.com/www.paulbirch.net/OrbitalRings-I.pdf

[6] K. Lofstrom, "The Launch Loop, A Low-Cost Earth-to-High-Orbit Launch System," 2009, Accessed: Oct. 08, 2022. [Online]. Available: http://launchloop.com

[7] J. M. Knapman, "High-Altitude Electromagnetic Launcher Feasibility," *https://doi.org/10.2514/1.16990*, vol. 22, no. 4, pp. 757–763, May 2012, doi: 10.2514/1.16990.

[8] J. Knapman, "Stability of the Space Cable," 2006. Accessed: Jul. 19, 2022. [Online]. Available: http://www.spacecable.org.uk/Stability%20IAC.pdf

[9] Robert L. Forward, *Indistinguishable From Magic*. Bean Publishing Enterprises, 1995.

[10] D. Gilbert, "On the Mathematical Theory of Suspension Bridges, with Tables for Facilitating Their Construction," *Philos Trans R Soc Lond*, vol. 116, no. 1/3, pp. 202–218, Sep. 1826.

[11] R. O. deCastongrene and R. F. Dominguez, "An investigation into the properties and characteristics of homogeneous tapered cables," *Tex A & M Univ Dep Civ Eng Rep COE-183*. 1975.

[12] W. J. Lewis, *Tension Structures: Form and Behaviour*. Thomas Telford, 2003.

[13] "Mars Helicopter - NASA Mars."

978-1-6654-9032-0/23/$31.00 ©2023 IEEE

https://mars.nasa.gov/technology/helicopter/#Tech-Specs (accessed Oct. 05, 2022).
[14] "A better approach to airline costs | McKinsey." https://www.mckinsey.com/industries/travel-logistics-and-infrastructure/our-insights/a-better-approach-to-airline-costs (accessed Oct. 12, 2022).
[15] P. Swan, "Tethered Ring Architectural Model, JavaScript and Three.js Repository on GitHub." https://github.com/philipswan/TetheredRing (accessed Jul. 16, 2022).
[16] "NASA Awards SpaceX More Crew Flights to Space Station | NASA." https://www.nasa.gov/feature/nasa-awards-spacex-more-crew-flights-to-space-station (accessed Oct. 13, 2022).
[17] Office of Inspector General, "Audit of Commercial Resupply Services To The International Space Station," Apr. 2018. Accessed: Aug. 10, 2022. [Online]. Available: https://oig.nasa.gov/docs/IG-18-016.pdf
[18] "IDV to SIERRA NEVADA CORPORATION | USAspending." https://www.usaspending.gov/award/CONT_IDV_NNJ16GX07B_8000 (accessed Jul. 16, 2022).
[19] "IDV to ORBITAL SCIENCES CORPORATION | USAspending." https://www.usaspending.gov/award/CONT_IDV_NNJ09GA02B_8000 (accessed Jul. 16, 2022).
[20] "IDV to SPACE EXPLORATION TECHNOLOGIES CORP. | USAspending." https://www.usaspending.gov/award/CONT_IDV_NNJ09GA04B_8000 (accessed Jul. 16, 2022).
[21] "P.47. Variable Step feed-screw in Fusion 360 /Шнек (Резьба) с переменным шагом во Fusion 360 - YouTube." https://www.youtube.com/watch?v=SI0qEBm8Z2U&ab_channel=EvgenRosta (accessed Oct. 11, 2022).
[22] "Janis | Cryogen-Free Superconducting Magnet Systems." https://www.lakeshore.com/products/product-detail/janis/cryogen-free-superconducting-magnet-systems (accessed Oct. 08, 2022).
[23] "Cryogen Free Superconducting Magnet Systems - Cryomagnetics." https://cryomagnetics.com/products/cryogen-free-superconducting-magnet-systems/ (accessed Oct. 08, 2022).
[24] "Cryogen Free Superconducting Magnet Systems".
[25] X. Li and A. Palazzolo, "A review of flywheel energy storage systems: state of the art and opportunities," *J Energy Storage*, vol. 46, Feb. 2022, doi: 10.1016/j.est.2021.103576.
[26] R. Hebner, "Low-Cost Flywheel Energy Storage for Mitigating the Variability of Renewable Power Generation".
[27] M. Osipov *et al.*, "Scalable superconductive magnetic bearing based on non-closed CC tapes windings," *Supercond Sci Technol*, vol. 34, no. 3, Mar. 2021, doi: 10.1088/1361-6668/ABDA5A.

10. BIOGRAPHY

Philip Swan *earned a Masters in Engineering from McGill University, Montreal in 1991, doing the thesis research at the Industrial Materials Research Institute of the National Research Council of Canada. He has a track record of developing successful innovations while working as a principal engineer on advanced multi-disciplinary projects including Xbox, Hololens, and Starlink. He has been granted 38 US patents.*

978-1-6654-9032-0/23/$31.00 ©2023 IEEE